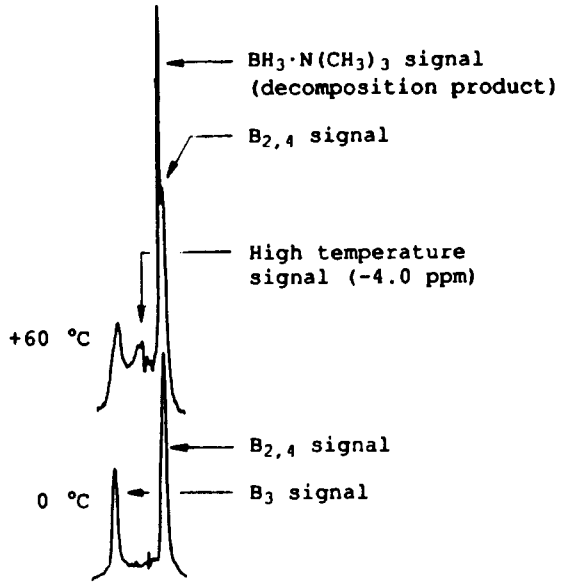

Figure 3. Portion of the $^{11}B\{^1H\}$ NMR spectrum (96.2 MHz) of $B_4H_8{\cdot}N(CH_3)_3$ showing the growth of the -4.0 ppm signal at the higher temperatures.

The diethyl etherate of boron trifluoride was used as the external standard for the ^{11}B shift values.

Isolation of $B_4H_8{\cdot}S(CH_3)_2$. A 0.453-mmol sample of B_5H_{11} was taken in a 9 mm o.d. Pyrex tube equipped with a Teflon valve and was dissolved in about a 2-mL sample of CH_2Cl_2. The solution was frozen at -197 °C, and a 0.983-mmol sample of $S(CH_3)_2$ was condensed into the tube. The tube was placed in a -80 °C bath, shaken to mix the contents thoroughly, and then placed in the cooled probe of the NMR spectrometer. The ^{11}B NMR spectrum of the solution contained only the signals of $BH_3{\cdot}S(CH_3)_2$ and $B_4H_8{\cdot}S(CH_3)_2$.

The tube was then placed in a -23 °C bath, and the volatile components were pumped out from the tube through a -63 °C trap into a -197 °C trap. From time to time, the liquid residue in the reaction tube was dissolved in a fresh, small portion of CH_2Cl_2 to record the ^{11}B NMR spectrum of the solution at -30 °C. A total pumping time of 30 h was required to remove $BH_3{\cdot}S(CH_3)_2$ completely from the product mixture. When the CH_2Cl_2 solution containing pure $B_4H_8{\cdot}S(CH_3)_2$ was kept at room temperature for a few minutes, the signal of $BH_3{\cdot}S(CH_3)_2$ became detectable.

Formation of $B_5H_{11}{\cdot}S(CH_3)_2$. A 0.150-mmol sample of B_5H_{11} was taken in a 14 mm o.d. Pyrex tube equipped with a vertical-shape Teflon valve (VNMR valve, product of J. Young Scientific Glassware) and was dissolved in a 2.0-mL sample of CH_2Cl_2. Then, the tube was placed in a -95 °C bath, and a 0.160-mmol sample of $S(CH_3)_2$ was slowly introduced over the B_5H_{11} solution, during which the solution was constantly agitated by shaking the tube in the bath. Then, the tube was inserted into the probe of a Varian XL-300 NMR spectrometer. The probe had been cooled to -100 °C prior to the insertion of the reaction tube. The spectrum obtained at -95 °C is shown in Figure 1. The probe temperature was increased to -80 °C and then to -60 °C in a stepwise fashion to record the spectra of the solution.

Sample Solutions for the Variable-Temperature NMR Studies. (a) $B_4H_8{\cdot}S(CH_3)_2$. The sample of $B_4H_8{\cdot}S(CH_3)_2$, which was prepared as described earlier in this section, was dissolved in a 2-mL sample of $S(CH_3)_2$. In a separate experiment, a 0.451 mmol sample of B_5H_{11} was dissolved in a 2-mL sample of $S(CH_3)_2$ at -80 °C. The formation of $B_4H_8{\cdot}S(CH_3)_2$ and $BH_3{\cdot}S(CH_3)_2$ was complete at this temperature. The $B_4H_8{\cdot}S(CH_3)_2$ signals of these two solutions showed identical changes with respect to the temperature variation.

(b) $B_4H_8{\cdot}S(C_2H_5)_2$ and $B_4H_8{\cdot}S(CH_2)_4$. The sample solution of $B_4H_8{\cdot}S(C_2H_5)_2$ was prepared in a 9 mm o.d. Pyrex tube by dissolving a 0.573-mmol sample of B_5H_{11} in a 2-mL sample of $S(C_2H_5)_2$ at -80 °C and raising the temperature slowly to -60°C. The sample solution of $B_4H_8{\cdot}S(CH_2)_4$ was prepared similarly by dissolving a 0.516-mmol sample of B_5H_{11} in a 2-mL sample of $S(CH_2)_4$.

(c) $B_4H_8{\cdot}P(CH_3)_3$. A 0.51-mmol sample of $B_4H_8{\cdot}P(CH_3)_3$, prepared in a 9 mm o.d. Pyrex tube by treating $B_4H_8{\cdot}2P(CH_3)_3$ with B_2H_6,[4b] was dissolved in a 1.5-mL sample of $S(CH_3)_2$. Another 0.52-mmol sample of $B_4H_8{\cdot}P(CH_3)_3$, which was similarly prepared, was dissolved in a 2-mL sample of $S(CH_2)_4$.

(d) $B_4H_8{\cdot}N(CH_3)_3$. A 0.68-mmol sample of $B_4H_8{\cdot}N(CH_3)_3$, prepared in a 9 mm o.d. Pyrex tube by the literature method,[4a] was dissolved in a 1.5-mL sample of $S(CH_3)_2$. After the completion of the measurements, the solvent $S(CH_3)_2$ was pumped out completely from the tube, and the remaining $B_4H_8{\cdot}N(CH_3)_3$ was dissolved in a 1.7-mL sample of $S(CH_2)_4$.

The ^{11}B NMR spectra of these sample solutions were recorded on the FT-80A spectrometer. The spectra of the $S(CH_2)_4$ solution of $B_4H_8{\cdot}N(CH_3)_3$ were also recorded on a Varian XL-300 spectrometer, so that the high-temperature signal at -4.0 ppm could be observed well-separated from the B_3 and $B_{2,4}$ signals, as shown in Figure 3. At +60 °C, decompositions of $B_4H_8{\cdot}N(CH_3)_3$ proceeded at an appreciable rate. However, the appearance–disappearance of the -4.0 ppm signal was reversible with respect to the temperature variation.

Acknowledgment. We gratefully acknowledge the support of this work by the U.S. Army Research Office through Grant DAAG 29-85-K-0034.

Contribution from the Departments of Chemistry, Rensselaer Polytechnic Institute, Troy, New York 12180, and King's College, Wilkes-Barre, Pennsylvania 18711

$Me_3Al{\cdot}NH_3$ Formation and Pyrolytic Methane Loss: Thermodynamics, Kinetics, and Mechanism

Frederick C. Sauls,*[1a] Leonard V. Interrante,*[1b] and Zhiping Jiang[1b]

Received December 14, 1989

The thermodynamics, kinetics, and mechanism of the reactions $Me_3Al + NH_3 \rightarrow Me_3Al{\cdot}NH_3 \xrightarrow{\Delta} {}^1/_3(Me_2AlNH_2)_3 + CH_4$ in homogeneous solution were investigated by solution calorimetry, DSC, and ^1H NMR rate measurements. The enthalpy for complex formation from NH_3 and monomeric Me_3Al in benzene was -93 kJ/mol. The observed ΔH for methane loss from the complex was -82.2 kcal/mol. Methane loss from $Me_3Al{\cdot}NH_3$ was catalyzed by excess Me_3Al monomer or monomeric Me_2AlNH_2 in equilibrium with $(Me_2AlNH_2)_2$ and $(Me_2AlNH_2)_3$. A mechanism for the Me_2AlNH_2-catalyzed reaction involving formation of the methyl-bridged intermediate $(\mu\text{-Me})(Me_2AlNH_2)(Me_2Al{\cdot}NH_3)$ and subsequent loss of CH_4 by proton transfer was proposed. The enthalpy of activation for the autocatalytic reaction was 92.8 kJ/mol. A deuterium isotope effect of 8.8 was measured for this reaction. A similar mechanism was proposed for the Me_3Al-catalyzed reaction, involving formation of an analogous methyl-bridged species $(\mu\text{-Me})(Me_3Al)(Me_2Al{\cdot}NH_3)$, which apparently loses CH_4 and closes to metastable $(\mu\text{-}NH_2)(\mu\text{-Me})Al_2Me_4$. This slowly disproportionates to $(Me_3Al)_2$ and $(Me_2AlNH_2)_3$; the autocatalytic path is thus slowed. $\Delta H^{\ddagger}$, for the Me_3Al-catalyzed pathway was 113 kJ/mol. The deuterium isotope effect was 5.5.

Introduction

A general route to nonoxide ceramic materials is the pyrolytic decomposition of a suitable organometallic precursor. While this approach has received considerable attention, the mechanisms of the underlying organometallic thermal elimination reactions have not. The elucidation of these reactions may prove important for the optimization of such ceramic generation processes; it is also essential for a full fundamental understanding of the chemistry

(1) (a) King's College. (b) Rensselaer Polytechnic Institute.

0020-1669/90/1329-2989$02.50/0

of the inorganic compounds and polymers used in these processes.

Organoaluminum compounds are known to form adducts with ammonia, which undergo the following series of reactions first elucidated by Wiberg in 1939:[2]

$$R_3Al + NH_3 \rightarrow \underset{\text{"adduct"}}{R_3Al{\cdot}NH_3} \xrightarrow{\Delta} \underset{\text{"amide"}}{(R_2AlNH_2)_{2\text{ or }3}} \xrightarrow{\Delta} \underset{\text{"imide"}}{(RAlNH)_n} \xrightarrow{\Delta} AlN \quad (1)$$

The final product AlN is a ceramic with attractive properties for electronic and structural applications.[3-8]

The nature of some of the amide and imide intermediates in the thermolytic conversion have subsequently been investigated and the results summarized.[9-14] Thermolysis of these amides or the adduct $Me_3Al{\cdot}NH_3$ in the absence of excess ammonia yields a black powder high in carbon; however, empirical modifications of this chemistry have yielded high-purity AlN.[15-18] An understanding of the decomposition mechanism would allow rational selection of substituents on Al and N; moreover, processing conditions to produce films or powders of appropriate purity and morphology or conditions compatible with on-chip device fabrication might be selected.

There have been few relevant kinetic studies of elimination from analogous compounds. Schleyer and Ring[19,20] studied the pyrolysis of $Me_3Ga + AsH_3$ and $Me_3Ga + PH_3$. Their work was done in the vapor phase at reduced pressures and focused on the surface-catalyzed decomposition to GaAs or GaP

$$Me_3Ga + AsH_3 \xrightarrow{\Delta} Me_{3-x}GaAsH_{3-x} + xCH_4 \quad (2)$$

They found no evidence for formation of $Me_3Ga{\cdot}AsH_3$ or $Me_3Ga{\cdot}PH_3$. The reaction could not be separated cleanly into steps, as can the $Me_3Al + NH_3$ reaction sequence. Their rate data indicate that loss of the first methane was catalyzed by the $Me_{3-x}GaAsH_{3-x}$ surface produced.

Beachley and co-workers studied the H_2-elimination kinetics in mixtures of $(Me_2AlH)_3$ with *N*-methylaniline, benzylamine, or methylphenylphosphine.[21-23] The processes appear to be complex, especially in the last system.

This paper reports the results of our study of the reactions

$$Me_3Al + NH_3 \rightarrow Me_3Al{\cdot}NH_3 \xrightarrow{\Delta} \tfrac{1}{3}(Me_2AlNH_2)_3 + CH_4 \quad (3)$$

We chose trimethylaluminum because the chemistry of the system has been investigated.[17] The NMR spectra are simple, and the resonances of interest are well separated, affording a convenient method of following the reaction. Moreover, trimethylaluminum cannot decompose via alkene loss to the corresponding aluminum hydride, avoiding a potential complication.

The reactivity of alkylaluminum compounds and their amine derivatives toward polar solvents and the very limited solubility of the amine derivatives in alkanes limit these studies to use of the neat compounds or to solution in aromatic solvents, e.g. benzene and toluene.

Experimental Section

All solution preparation and handling of alkylaluminum compounds were done in a N_2-filled drybox or in Schlenk glassware under N_2, respecting their sensitivity to oxygen and moisture.[24]

$(Me_3Al)_2$ and $(Et_3Al)_2$ (Texas Alkyls), $(Me_3Al)_2$ (electronic grade, Alfa Inorganics), ND_3 (99.5% D, Cambridge Isotope Laboratories), NH_3 (electronic grade, Matheson), and benzene-d_6 and toluene-d_8 (99.5%, and 99% D respectively, Aldrich) were used as received. NH_3 (USS Agri-Chemicals) was dried over Na before use. NH_2Me (Matheson) was dried by passage over KOH. Pentane (Fisher) was distilled from CaH_2 under N_2; benzene and toluene (Fisher) were distilled from Na under N_2.

$Me_3Al{\cdot}NH_3$ was prepared by bubbling NH_3 for 3 h through a solution of 25 mL of $(Me_3Al)_2$ and 75 mL of pentane in a dry ice/2-propanol bath. Pentane and excess NH_3 were removed in vacuo at room temperature overnight. The white solid was stored at −30 °C, as it decomposes in a few days at room temperature. NMR measurements indicate the presence of ca. 5% $(Me_2AlNH_2)_3$ in the resulting product. $Me_3Al{\cdot}ND_3$ was prepared in identical fashion from ND_3, 2 mL of $(Me_3Al)_2$ and 6 mL of pentane; it contained ca. 2% $(Me_2AlND_2)_3$. High-purity $Me_3Al{\cdot}NH_3$ was prepared by condensing electronic-grade NH_3 into electronic-grade $(Me_3Al)_2$ with stirring for several hours at −78 °C, then removing the excess NH_3 under vacuum at −78 °C. This material contained no $(Me_2AlNH_2)_3$ detectable by ^1H NMR. Kinetic results reported here were obtained using the high-purity product. However, allowing for the $(Me_2AlNH_2)_3$ present in the first preparation, no difference in the kinetic properties of $Me_3Al{\cdot}NH_3$ prepared by the two methods was detected. This suggests that any trace impurities present are probably not kinetically significant. $(Me_2AlNH_2)_3$,[17] $[Me_2AlNHMe]_3$,[25] and $[Et_2AlNH_2]_3$[17] were prepared as described.

Calorimetric measurements were made in the drybox, using a Parr Model 1451 Solution Calorimeter, calibrated as recommended by the manufacturer.[26] The heat capacity of benzene was taken to be 1.73 J/(g °C).[27] Trimethylaluminum (ca. 0.5 g, 3.5 mmol) was added to weighed amounts (ca. 85 g) of benzene in the calorimeter Dewar flask, and thermal equilibration was allowed. (All weighings were carried out to the nearest milligram.) Sodium-dried NH_3 was then passed into the solution at approximately 10 mL/min. Exothermic complexation caused a linear (slope A) temperature rise. The extent of this rise was used to compute the heat of reaction. When the reaction was complete, a sharp transition to lesser slope (slope B) occurred, due to exothermic solution of NH_3 in benzene. The heat of solution of NH_3 in benzene (which does not appear to have been reported)[28] was obtained as the product of the heat of reaction and (slope B/slope A). The temperature eventually leveled and showed a decrease after the solution became saturated with NH_3 and escaping bubbles removed benzene vapor. Runs without trimethylaluminum showed identical behavior, without the initial slope due to the complexation reaction.

Differential scanning calorimetry was performed on a Perkin-Elmer 7 Series Thermal Analysis System. $Me_3Al{\cdot}NH_3$ was analyzed in a sealed

(2) Work of E. Wiberg, reported in: Bahr, G. In *Inorganic Chemistry, Part 2*; Klemm, W., Ed.; FIAT Review of WWII German Science; 1948; Vol. 24, p 155.
(3) Slack, G. A.; Tanzilli, R. A.; Pohl, R. O.; Vandersande, J. W. *J. Phys. Chem. Solids* **1987**, *48*, 641.
(4) Kuramato, N.; Taniguchi, H. *J. Mater. Sci. Lett.* **1984**, *3*, 471.
(5) Slack, G. A.; McNelly, T. F. *J. Cryst. Growth* **1976**, *34*, 263.
(6) Slack, G. A.; Bartram, S. F. *J. Appl. Phys.* **1975**, *46*, 89.
(7) Slack, G. A.; McNelly, T. F. *J. Cryst. Growth* **1977**, *42*, 550.
(8) Slack, G. A. *J. Phys. Chem. Solids* **1973**, *34*, 321.
(9) Mole, T.; Jeffrey, E. A. *Organoaluminum Compounds*; Elsevier: Amsterdam, 1972, p 229.
(10) Lappert, M. F.; Power, P. P.; Sanger, A. R.; Srivastava, R. C. *Metal and Metalloid Amides*; Wiley: New York, 1980; p 99.
(11) Eisch, J. J. Aluminum. In *Comprehensive Organometallic Chemistry*; Wilkinson, G., Ed.; Pergamon: Oxford, England, 1982; Vol. 1, p 555.
(12) Taylor, M. J. Aluminum and Gallium. In *Comprehensive Organometallic Chemistry*; Wilkinson, G., Ed.; Pergamon: Oxford, England, 1987; Vol. 3, p 107.
(13) Cesari, M.; Cucinella, S. Aluminum-Nitrogen Rings and Cages. In *The Chemistry of Inorganic Homo- and Heterocycles*; Haiduc, I., Sowerby, D. B., Eds.; Academic Press: London, 1987; p 167.
(14) Interrante, L. V.; Sigel, G. A.; Garbauskas, M.; Hejna, C.; Slack, G. A. *Inorg. Chem.* **1989**, *28*, 252.
(15) Tebbe, F. N.; Bolt, J. D.; Young, R. Y., Jr.; Van Buskirk, O. R.; Mahler, W.; Reddy, G. S.; Chowdhry, U. Thermoplastic Organoaluminum Precursor of Aluminum Nitride. In *Proceedings of Advances in Ceramics*; O'Bryan, H. M., Niwa, K., Young, W., Yan, M. S., Eds; American Chemical Society: Columbus, OH; Vol. 26, in press.
(16) Bolt, J. D.; Tebbe, F. N. Aluminum Nitride Fibers; Sintering and Microstructure. In *Proceedings of Advances in Ceramics*; O'Bryan, H. M., Niwa, K., Young, W., Yan, M. S., Eds.; American Ceramic Society: Columbus, OH, Vol. 26; in press.
(17) Interrante, L. V.; Carpenter, L. E.; Whitmarsh, C.; Lee, W.; Slack, G. A. *Mater. Res. Soc. Proc.* **1986**, *73*, 359.
(18) Interrante, L. V.; Lee, W.; McConnell, M.; Lewis, N.; Hall, E. *J. Electrochem. Soc.* **1989**, *132*, 472.
(19) Schleyer, D. J.; Ring, M. A. *J. Organomet. Chem.* **1976**, *114*, 9.
(20) Schleyer, D. J.; Ring, M. A. *J. Electrochem. Soc.* **1977**, *124*, 569.
(21) Beachley, O. T., Jr.; Tessier-Youngs, C. *Inorg. Chem.* **1979**, *18*, 3188.
(22) Beachley, O. T., Jr. *Inorg. Chem.* **1981**, *20*, 2825.
(23) Beachley, O. T., Jr.; Victoriano, L. *Inorg. Chem.* **1986**, *25*, 1948.
(24) (a) *Handling Procedures for Aluminum Alkyl Compounds and Other Organometallics*; Ethyl Corp.: Baton Rouge, LA. (b) Aluminum Alkyls ... Safety and Handling; Texas Alkyls, Inc.: Deer Park, TX.
(25) Alford, K. J.; Gosling, K.; Smith, J. D. *J. Chem. Soc., Dalton Trans.* **1972**, 2203.
(26) *Instructions for the 1451 Solution Calorimeter*; Parr Instrument Co.: Moline, IL.
(27) Shaw, R. *Chem. Eng. Data* **1969**, *14*, 461.
(28) Kerles, A. S. Ed. *IUPAC Solubility Data Series*; Pergamon: Oxford, England, 1985; Vol. 21, p 3.

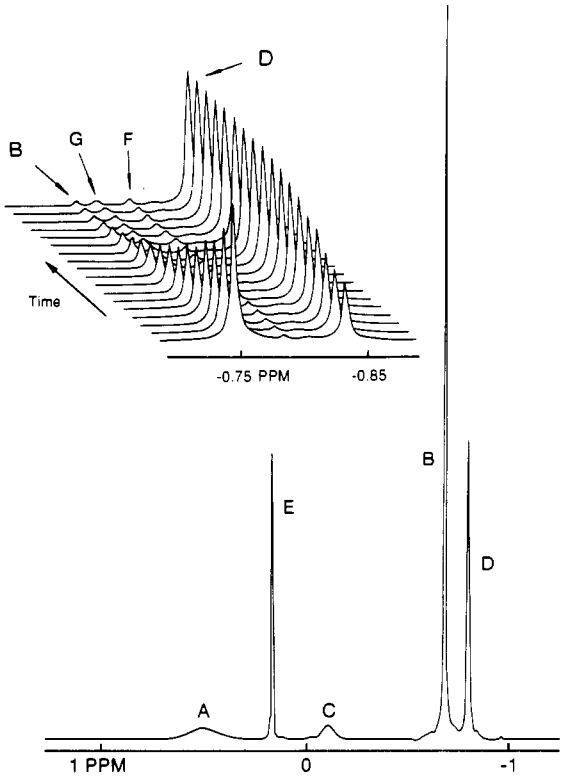

Figure 1. ^1H NMR spectrum of partially decomposed $Me_3Al{\cdot}NH_3$ in benzene-d_6. Inset: methyl region as decomposition proceeds. Assignments: $Me_3Al{\cdot}NH_3$, A = N–H, B = Me; $(Me_2AlNH_2)_3$, C = N–H, D = Me; methane, E; (Me_2AlNH_2), F = Me; impurity, G.

stainless-steel pan by heating from ambient temperature at 2.0 °C/min. Activation energy and reaction order were determined from the relationship[29]

$$k = (dH/dt)(m_0/H_0)m^x \qquad (4)$$

where k = rate constant, dH/dt = heat flow rate, m_0 = original sample mass, H_0 = total heat flow, m = mass of unreacted sample, and x = reaction order. A plot of ln k vs $1/T$ gave the activation energy.

^1H NMR measurements were made on a Varian XL-200 magnetic resonance spectrometer at 200 MHz, using residual protons in deuteriobenzene (δ = 7.15 ppm) or residual α-protons in deuteriotoluene (δ = 2.09 ppm) as reference. TMS was not added to the samples, as its resonance overlaps other peaks of interest. T_1 values for the methyl protons of $Me_3Al{\cdot}NH_3$ and $(Me_2AlNH_2)_3$ were 0.1 s in 0.1 M solution at room temperature. (At higher temperatures decomposition causes the concentrations to vary with time, making T_1 determinations difficult.) An interpulse delay of 3 s was used at all temperatures in order to assure accurate quantitation. Several kinetics runs were repeated using 1-s delays in order to test the validity of this procedure; no change in the kinetic results were noted. All reported results were obtained by using the 3-s delay.

Solutions of alkylaluminum compounds for kinetics runs were prepared gravimetrically in benzene-d_6 with initial concentrations of 0.02–0.5 M. Lower concentrations gave inadequate S/N for acceptable quantitation; higher concentrations generated excessive methane pressure when decomposed within the NMR tube.

For all solutions except those containing excess $(Me_3Al)_2$ the kinetic runs were performed as follows. Solutions of varying initial [$Me_3Al{\cdot}NH_3$] and [$(Me_2AlNH_2)_3$] in benzene-d_6 were prepared and their decompositions according to reaction 3 were followed by ^1H NMR at various temperatures between 35 and 80 °C. The area of the peak due to the methyl group of reactant $Me_3Al{\cdot}NH_3$ (B) and that of the product $(Me_2AlNH_2)_3$ (D), as shown in Figure 1, were measured. Some samples were followed to greater than 95% decomposition. The fraction of reactant remaining was computed as Fr = $B/(B + 1.5D)$.

Series in which the ammonia concentration was varied were prepared by weighing the aluminum compound into the solvent and dividing the solution into two portions. One portion was saturated with ammonia (ca. 2 M). Mixing these solutions in different proportions produced a series

(29) Wendlandt, W. W. *Thermal Methods of Analysis*, 3rd ed.; Wiley: New York, 1980; p 282.

Scheme I. Summary of the Decomposition of $Me_3Al{\cdot}NH_3$

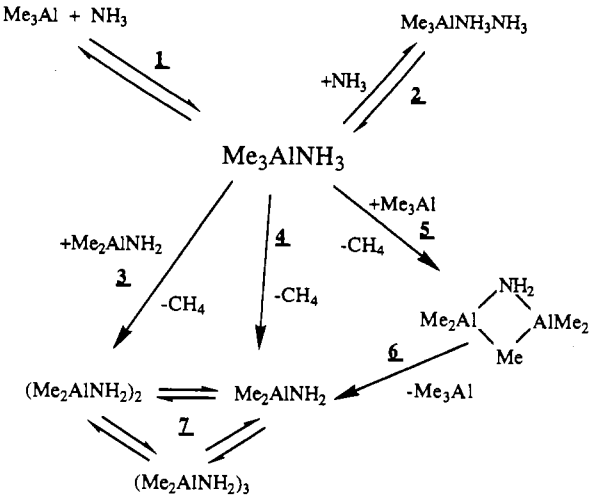

with a constant alkylaluminum concentration but varying ammonia concentrations. Integration of the Al–methyl and N–H regions of the NMR spectra allowed their ratio to be computed. The width of the N–H peaks rendered integration inaccurate; the resulting uncertainty in [NH_3] contributes to the scatter in Figure 7. Kinetics runs on these solutions were performed as above in random order to minimize the effect of any ammonia loss.

In the presence of excess $(Me_3Al)_2$ the reaction rate cannot be followed by integration of reactant and product peaks, as a metastable compound forms which has a resonance overlapping that of the adduct. The initial rate of reaction was determined as follows. A series of solutions containing 0.081 M $Me_3Al{\cdot}NH_3$ and varying amounts of $(Me_3Al)_2$ were prepared and decomposed at 55 °C. The initial rate of decomposition for each solution was followed by measuring the heights of the sharp CH_4 product peak and the residual solvent proton peak, as internal standard, at various times. (Accurate integration was not possible due to overlap of the CH_4 by the broad N–H resonance.) The initial rate of decomposition was then proportional to the initial slope of the $I(CH_4)/I$(benzene) vs time plot. The relative rate of initial methane loss from a sample containing no excess $(Me_3Al)_2$ was determined by an identical procedure for comparison purposes (the initial point in Figure 9).

The rate of CH_3D loss from the deuterated adduct in the presence of excess $(Me_3Al)_2$ was determined by similarly following the decomposition, allowing for the difference in product (CH_4 gives a singlet, 4 H; CH_3D gives a 1:1:1 triplet, 3 H). Any NOE due to the deuterium lock irradiation would cause a relative increase in the CH_3D signal. T_1 for CH_3D would be expected to be less than T_1 for CH_4, also tending to increase the CH_3D signal relative to that of CH_4. Thus errors from these sources would decrease R_H/R_D and lead to an underestimate of the isotope effect.

As only the initial part of the reaction is monitored, the [CH_4] in solution is well below saturation and bubbles do not form. Variations in field homogeneity will affect the peak height of both methane and the internal standard similarly; errors due to this source should largely cancel. Equilibration between solution and gas may be incomplete, and is probably the cause of much of the scatter in Figure 9. Although the relative rate measurements obtained with this method are clearly less precise than those obtained by integrating product and reactant peaks, they are sufficiently accurate for the purposes required.

Temperatures were measured before and after each kinetics run by inserting a sealed methanol or ethylene glycol sample into the spectrometer probe, allowing thermal equilibration, and measuring the peak separation. An internal program computed the temperature using van Geet's equations.[30] The average of the two determinations, which differed by less than 0.5 °C, was taken to be the sample temperature. For each series of kinetics runs the temperatures were varied in random fashion over the range of interest (35–80 °C).

Results and Discussion

Our principal conclusions on the reactions of $Me_3Al{\cdot}NH_3$ in aromatic solvents are summarized in Scheme I. The data supporting our conclusions will be discussed in sections labeled according to the numbers in Scheme I.

(30) van Geet, A. L. *Anal. Chem.* **1968**, *40*, 2227.

A. Adduct Formation (Path 1). When NH_3 is passed into $(Me_3Al)_2$, either neat or in solution, Me_3AlNH_3 is rapidly formed. Our experimental values for the heat of solution of ammonia in benzene and for the reaction

$$\tfrac{1}{2}(Me_3Al)_2\ (\text{benzene}) + NH_3(g) \rightarrow Me_3Al{\cdot}NH_3\ (\text{benzene}) \quad (5)$$

are -12 ± 4 and -72 ± 3 kJ/mol, respectively. The heat of dissociation of $(Me_3Al)_2$ in hexadecane solution[31] and the estimated value of the heat of complexation of Me_3Al monomer with benzene[32] in hexadecane are 81.2 ± 1.3 and -8 kJ/mol, respectively. Combining these values gives $\Delta H = -93 \pm 5$ kJ/mol for the coordination reaction

$$Me_3Al\ (\text{benzene}) + NH_3\ (\text{benzene}) \rightarrow Me_3Al{\cdot}NH_3\ (\text{benzene}) \quad (6)$$

Henrickson et al.[33] have determined $\Delta H = -115.3$ kJ/mol for the same reaction in hexane, but it is unclear whether the product remained in solution or precipitated as the solid.

B. Adduct Interactions with Alkylaluminum and Amines (Paths 1 and 2). NMR spectra of a solution of $Me_3Al{\cdot}NH_3$ ($\approx$0.1 M) in toluene-d_8 show a steady upfield movement of the N–H proton signal as temperature decreases from +80 to −90 °C. An opposite shift would be expected for increased $Me_3Al + NH_3$ association as temperature decreases. Instead, this is attributed to the formation of a weak complex between the aromatic π cloud and the relatively positive N–H protons, causing a shielding effect.[34] This complexation also explains the adduct's much higher solubility in aromatic solvents than in alkanes.

$Me_3Al{\cdot}NH_3$ and $(Me_3Al)_2$ ($\approx$0.1 M each in benzene-d_6 solution, 10–80 °C) show two separate methyl resonances at −0.74 and −0.35 ppm, respectively, indicating that exchange is slow on the NMR time scale. In contrast, for a solution of $Me_3Al{\cdot}NH_3$ ($\approx$0.1 M) in excess NH_3 ($\approx$0.3 M), only one N–H signal is seen; exchange must be rapid on the NMR time scale. Analogous solutions containing $Me_3Al{\cdot}NH_2Me$ and excess NH_2Me show only one N–H and one set of N–Me peaks, even when cooled to −90 °C in toluene-d_8, also demonstrating rapid exchange. Since the exchange of methyl groups on nitrogen is improbable, we conclude that whole-molecule exchange of coordinated amine is rapid down to −90 °C. Below ca. −30 °C, coupling between N–H and N–Me appears in the presence of excess amine, indicating that proton exchange becomes slow on the NMR time scale under these conditions. This indicates that whole-molecule amine exchange is more facile than proton exchange. N–H shifts are similar to those for the ammonia complex, indicating similar π-complexes and hydrogen bonding.

Since exchange is much more rapid in the presence of excess amine than with excess $(Me_3Al)_2$, the process is probably associative, as proposed by Mole and Jeffrey.[35]

C. Monomer–Dimer–Trimer Equilibrium (Path 7). The small peak 0.1 ppm downfield from the $(Me_2AlNH_2)_3$ methyl peak (cf. Figure 1 inset) was noted to vary in relative height with total amide concentration and to increase reversibly with temperature, indicating the species responsible to be in equilibrium with the trimer. Solutions of varying total $(Me_2AlNH_2)_x$ concentration were prepared, the peak heights were measured, and the equilibrium constant for the reaction

$$2(Me_2AlNH_2)_3 \overset{K_{32}}{\rightleftharpoons} 3(Me_2AlNH_2)_2 \quad (7)$$

was computed. (The small value of K_{32} precluded its determination by molecular weight measurements.) Determination of K_{32} at temperatures of 40–80 °C allowed calculation of ΔH. K_{32} is 1×10^{-5} at 80 °C; ΔH is 38 kJ for the reaction as written. Equilibration is rapid compared with methane loss from the adduct, which supports the assumption of rapid equilibration made below in the rate law interpretation. Details are reported elsewhere.[36]

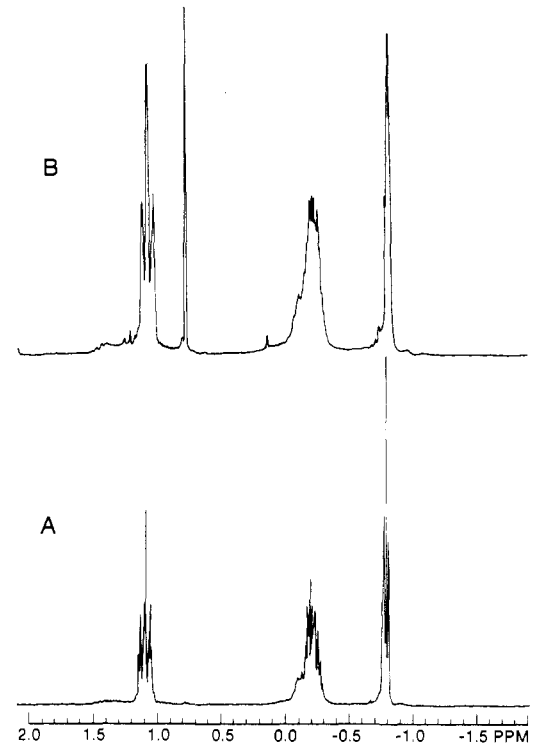

Figure 2. A. ^1H NMR spectrum of $(Et_2AlNH_2)_3$ and $(Me_2AlNH_2)_3$ mixture in benzene-d_6 after heating for 10 min at 80 °C. Four species, $(Et_2AlNH_2)_3$, $(Et_2AlNH_2)_2Me_2AlNH_2$, $Et_2AlNH_2(Me_2AlNH_2)_2$, and $(Me_2AlNH_2)_3$, give three distinct and resolved methyl and ethyl environments. B. ^1H NMR spectrum of $(Et_2AlNH_2)_3$ and $Me_3Al{\cdot}NH_3$ mixture in benzene-d_6 after heating for 10 min at 80 °C. Alkyl scrambling yields the mixture of products $((Me,Et)_2AlNH_2)_3$ containing nine different species whose resonances are not resolved, along with ethane and a very small amount of methane.

Mixing of $(Me_2AlNH_2)_3$ and $(Et_2AlNH_2)_3$ ($\approx$0.1 M each in benzene-d_6, less than 30 min at ambient temperature) produces only partial scrambling; i.e., Et_2Al and Me_2Al units remain intact, and no EtMeAl units are produced (Figure 2A). Heating to 80 °C for an hour still produces no EtMeAl units. This is consistent with dissociation into Et_2AlNH_2 and Me_2AlNH_2 monomers, which randomly combine. As this exchange is also faster than methane loss from the adduct, the assumption of rapid equilibrium made below is further supported.

There are, of course, other mechanisms that can account for these exchanges. Our principal justification for assuming the presence of Me_2AlNH_2 monomers is the rate law given in part D. It is interesting to note that the analogous Me_2BNH_2 is a dimer below 30 °C but a monomer at higher temperatures.[37]

D. Decomposition (Paths 3–5). DSC measurements show that $\Delta H = -82.2$ kJ/mol for methane loss from the adduct:

$$Me_3Al{\cdot}NH_3(l) \xrightarrow{\Delta} \tfrac{1}{3}(Me_2AlNH_2)_3(l) + CH_4(g) \quad (8)$$

Our experimental rate law suggests that this decomposition process takes place via two routes, one catalyzed by free Me_3Al and one by monomeric Me_2AlNH_2.

$$Me_3Al{\cdot}NH_3 + Me_3Al \xrightarrow{k_1} Me_2AlNH_2{\cdot}Me_3Al + CH_4 \quad (9)$$

$$Me_3Al{\cdot}NH_3 + Me_2AlNH_2 \xrightarrow{k_2} (Me_2AlNH_2)_2 + CH_4 \quad (10)$$

The rate law for this two-path mechanism is

(31) Smith, M. B. *J. Organomet. Chem.* **1972**, *46*, 31.
(32) Reference 11, p 593.
(33) Henrickson, C. H.; Duffy, D.; Eyman, D. P. *Inorg. Chem.* **1968**, *7*, 1047.
(34) Ronayne, J.; Williams, D. H. *Annu. Rev. NMR Spectrosc.* **1969**, *2*, 83.
(35) Reference 9, p 114.
(36) Sauls, F. C.; Czekaj, C. L.; Interrante, L. V. Submitted for publication in *Inorg. Chem.*
(37) Wiberg, E.; Hertwig, K.; Boltz, A. *Z. Anorg. Chem.* **1948**, *256*, 177.

$$R = -d[Me_3Al{\cdot}NH_3]/dt$$
$$= k_1[Me_3Al{\cdot}NH_3][Me_3Al] + k_2[Me_3Al{\cdot}NH_3][Me_2AlNH_2] \quad (11)$$

If we assume the rapid dissociation equilibria

$$Me_3Al{\cdot}NH_3 \overset{K_1}{\rightleftharpoons} Me_3Al + NH_3 \quad K_1 \ll 1 \quad (12)$$

$$^1/_3(Me_2AlNH_2)_3 \overset{K_{31}}{\rightleftharpoons} Me_2AlNH_2 \quad K_{31} \ll 1 \quad (13)$$

the rate law then becomes

$$R = k_1K_1^{1/2}[Me_3Al{\cdot}NH_3]^{3/2} + k_2K_{31}[Me_3Al{\cdot}NH_3][(Me_2AlNH_2)_3]^{1/3} \quad (14)$$

Plots of ln (Fr) vs time for solutions containing varied initial concentrations of $Me_3Al{\cdot}NH_3$ and $(Me_2AlNH_2)_3$ are shown in Figures 3 and 4. Solid lines show the results obtained from the proposed rate law (eq 14), with $k_1K_1^{1/2} = 5.5 \times 10^{-4}$ and $k_2K_{31} = 1.5 \times 10^{-3}$.

Attempts to fit the data to single-term rate laws failed, demonstrating that the reaction is not simply n order in reactant. Rate laws containing several terms of different power in reactant, appropriate to a multipath but uncatalyzed mechanism, also fail to fit our results.

The observed value of $^3/_2$ for the first exponent in eq 14 eliminates both eq 12 as a rate-determining step (an exponent of 1 would be required) and $(Me_3Al)_2$ as catalyst (requires an exponent of 2). The experimental value of $^1/_3$ for the second exponent in eq 14 eliminates eq 13 as rate-determining (exponent of 1 required) as well as $(Me_2AlNH_2)_{2\text{ or }3}$, either in cyclic or ring-opened forms, as catalyst ($^2/_3$ or 1 required).

The extent of $Me_3Al{\cdot}NH_3$ dissociation must be small, as Me_3AlNH_3 in solution shows no sign of a peak due to free $(Me_3Al)_2$. A peak 10% of the principal peak in 0.01 M solution would have been easily discernible. This yields $K_1 < 10^{-4}$ at 20 °C. ΔH^* for dissociation must of course equal or exceed 93 kJ/mol.

E. Me_2AlNH_2-Catalyzed Decomposition (Path 3). We consider the decomposition of a solution of Me_3AlNH_3, and rearrange the rate law (eq 14) to

$$R = (k_1K_1^{1/2}[Me_3Al{\cdot}NH_3]^{1/2} + k_2K_{31}[(Me_2AlNH_2)_3]^{1/3})[Me_3Al{\cdot}NH_3] \quad (15)$$

In the later portion of the decomposition the reaction is dominated by the Me_2AlNH_2-catalyzed pathway, as $k_1K_1^{1/2}$ and $[Me_3Al{\cdot}NH_3]$ are both small. The first term in the parentheses becomes insignificant, and the rate law in this region becomes

$$R \approx k_2K_{31}[(Me_2AlNH_2)_3]^{1/3}[Me_3Al{\cdot}NH_3] = k_{ps}[Me_3Al{\cdot}NH_3] \quad (16)$$

Recognizing that in this region decomposition is largely complete, $[(Me_2AlNH_2)_3]$ is approximately equal to the initial $[(Me_2AlNH_2)_3]$ plus one-third the initial $[Me_3Al{\cdot}NH_3]$ and varies but little with time. The reaction thus becomes pseudo-first order in $Me_3Al{\cdot}NH_3$ with

$$k_{ps} = k_2K_{31}(^1/_3[Me_3Al{\cdot}NH_3]_{init} + [(Me_2AlNH_2)_3]_{init})^{1/3} \quad (17)$$

This implies that the plots of ln (Fr) vs time should become linear in the latter portion, as decomposition is largely complete. The limiting slope (k_{ps}) should vary with the initial concentrations according to eq 17. This prediction is confirmed in Figure 5. A series of solutions with varying initial $[Me_3Al{\cdot}NH_3]$ and $[(Me_2AlNH_2)_3]$ was prepared and their decompositions monitored. k_{ps} is seen to be linear in the quantity $\{^1/_3[Me_3Al{\cdot}NH_3]_{init} + [(Me_2AlNH_2)_3]_{init}\}^{1/3}$.

$Me_3Al{\cdot}NH_3$ (0.2 M) was decomposed in benzene-d_6 at various temperatures. A plot of ln k_{ps} vs $1/T$ (Figure 6) gave ΔH^* of 92.8 ± 1.2 kJ/mol. Identical measurements with $Me_3Al{\cdot}ND_3$ gave ΔH^* of 109 ± 2.5 kJ/mol. Direct comparison of solutions of identical concentrations gave a deuterium isotope effect of 8.8 at 67.2 °C. Substitution of D for H would not be expected to alter K_{31} significantly in aromatic solvents; these results thus indicate substantial N–H bond breaking at the transition state.

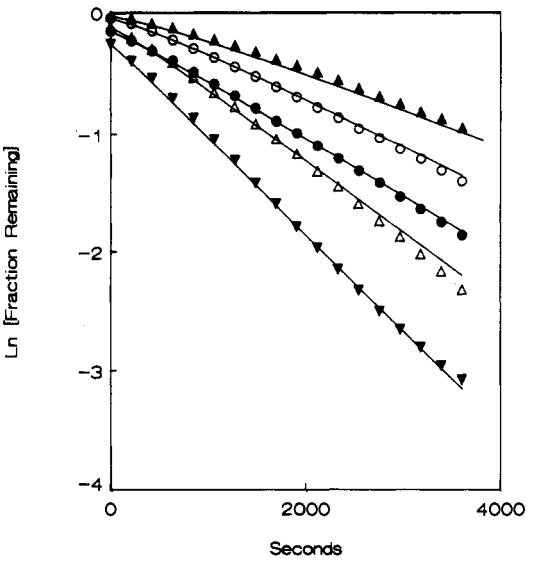

Figure 3. Plots of ln(fraction remaining) [ln (Fr)] vs time at 61.5 °C for solutions containing varied initial concentrations of $Me_3Al{\cdot}NH_3$ and $(Me_2AlNH_2)_3$, respectively: (▲) 0.0214, 0.002 M; (○) 0.0414, 0.0007 M; (●) 0.0614, 0.0034 M; (△) 0.11, 0.0046 M; (▼) 0.2117, 0.0207 M. The solid lines were computed by using the proposed rate law.

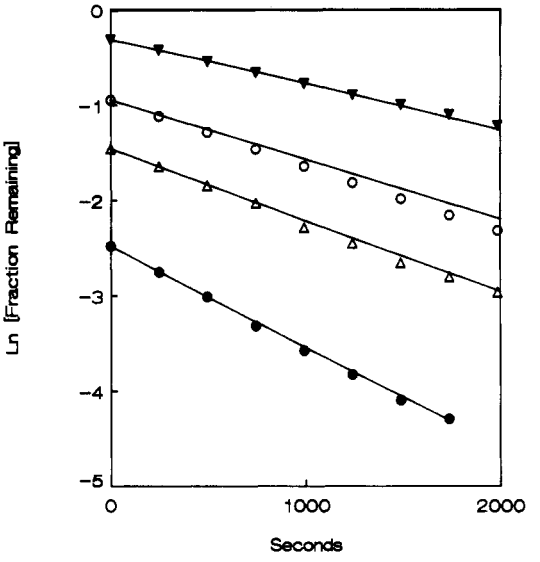

Figure 4. Plots of ln (Fr) vs time at 61.5 °C for solutions containing 0.0565 M $Me_3Al{\cdot}NH_3$ and varied concentrations of $(Me_2AlNH_2)_3$: (▼) 0.0057 M; (○) 0.0251 M; (△) 0.0592 M; (●) 0.182 M. The solid lines were computed by using the proposed rate law.

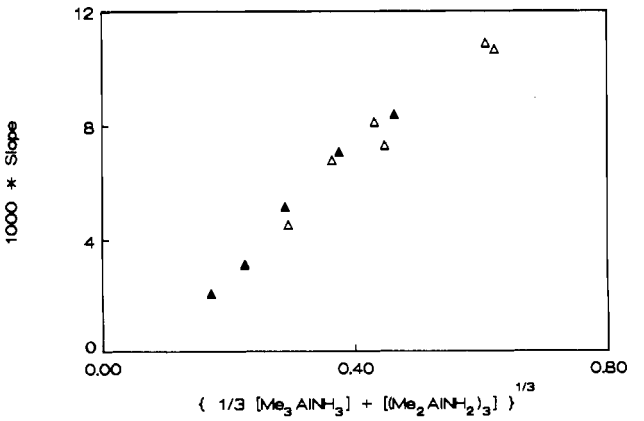

Figure 5. Test for pseudo-first-order behavior. For ▲ the initial concentrations were those of Figure 3, and for △, those of Figure 4.

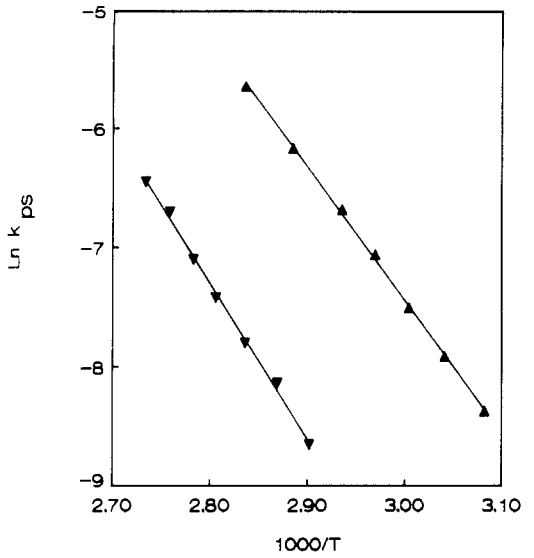

Figure 6. Determination of $\Delta H^{\ddagger}$ for the catalyzed methane loss from $Me_3Al{\cdot}NH_3$. k_{ps} is the pseudo-first-order rate constant. All solutions were initially 0.2 M in $Me_3Al{\cdot}NH_3$ (▲) or $Me_3Al{\cdot}ND_3$ (▼).

The rate law implies that the transition state for the Me_2AlNH_2-catalyzed pathway contains one Me_2AlNH_2 and one $Me_3Al{\cdot}NH_3$. The isotope effect suggests that N–H bond breaking is important.

We postulate that the Me_2AlNH_2-catalyzed methane loss begins with formation of a methyl bridge between the adduct methyl group and the empty p_z orbital of the Me_2AlNH_2 (step A). The highly acidic N–H then attacks the nearby electron-rich methyl group, which departs as methane (steps B and C). The nitrogen lone pair forms a bond with the empty aluminum orbital, yielding a methyl-bridged ring (step D), which then rearranges to the more stable amido-bridged form (step E).

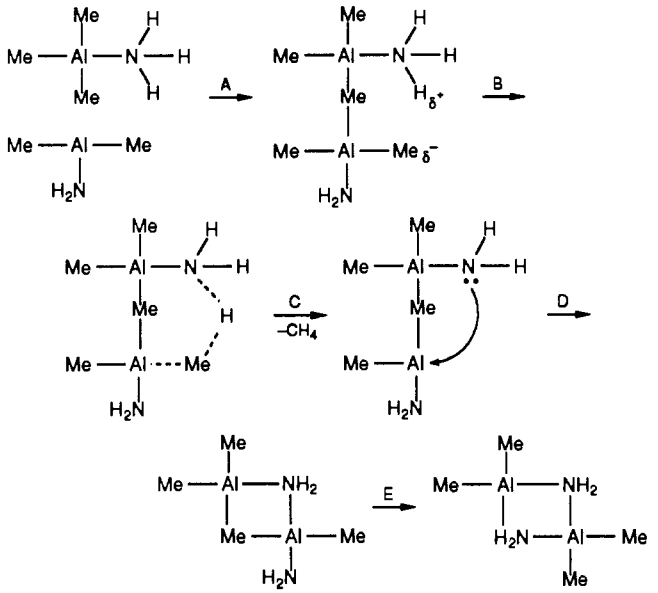

Mechanisms involving initial attack of the catalyst on the adduct nitrogen are less plausible, as this nitrogen bears a significant positive charge and is therefore less attractive to the Lewis acid catalyst.

Excess ammonia slows the Me_2AlNH_2-catalyzed reaction by a factor of up to 3 (Figure 7). $\Delta H^{\ddagger}$ appears to increase slightly (from 92.8 to 98.4 kJ/mol) in going from no excess NH_3 to approximately a 5-fold excess. This could be due to H bonding between the very positive adduct N–H protons and the ammonia lone pair or because the excess NH_3 forms a complex with the monomeric amide catalyst.

By DSC measurements an activation enthalpy of 174 kJ/mol and order = 1 were found for the decomposition of the neat liquid

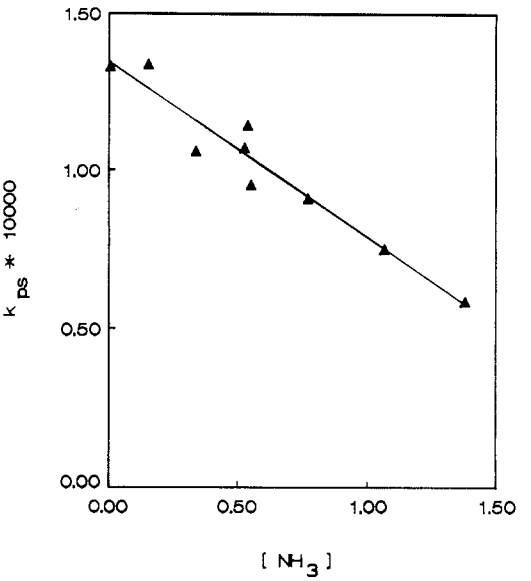

Figure 7. Influence of NH_3 on the Me_2AlNH_2-catalyzed methane loss from $Me_3Al{\cdot}NH_3$ at 51.7 °C. Initial $[Me_3Al{\cdot}NH_3]$ was ca. 0.1 M.

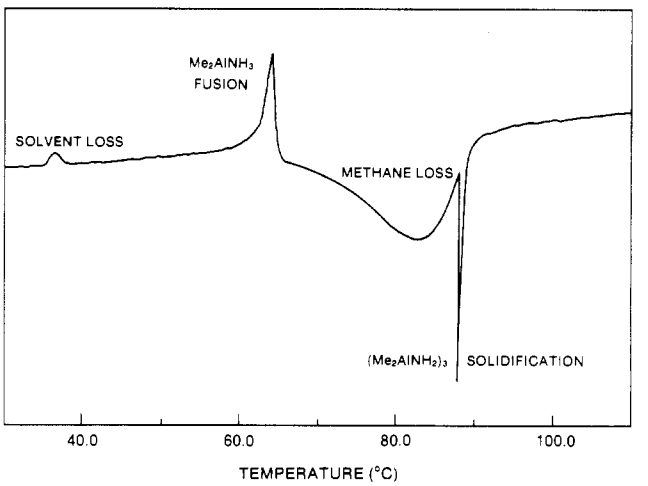

Figure 8. DSC for $Me_3Al{\cdot}NH_3$ heated at 2 °C/min in a sealed stainless-steel pan.

$Me_3Al{\cdot}NH_3$. This should correspond to the Me_2AlNH_2-catalyzed decomposition. The substantially larger activation enthalpy obtained compared to the value in benzene solution could be related to the difference in the reaction medium; however, the DSC values in this case are subject to substantial positive errors due to overlap of both the endothermic $Me_3Al{\cdot}NH_3$ fusion with the early part of the decomposition, and the exothermic $(Me_2AlNH_2)_3$ solidification with the latter part (Figure 8). We therefore have less confidence in this determination.

F. Alkyl Exchange. If a solution containing $Me_3Al{\cdot}ND_3$ and $(Me_2AlND_2)_3$ in toluene-d_8 is heated to 110 °C, the methyl resonances broaden and begin to coalesce, demonstrating fast exchange—much faster than the loss of CH_3D. (The deuterated compound and toluene solvent are required to slow the decomposition and to allow a higher temperature.) A natural modification of the previous mechanism explains this result. Rotation of the Me_2AlNH_2 about the methyl bridge leads to a slightly different geometry. H^+ transfer and subsequent dissociation yield simultaneous methyl and hydrogen exchange, in effect interchanging the identities of adduct and amide.

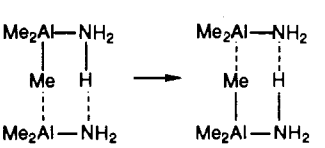

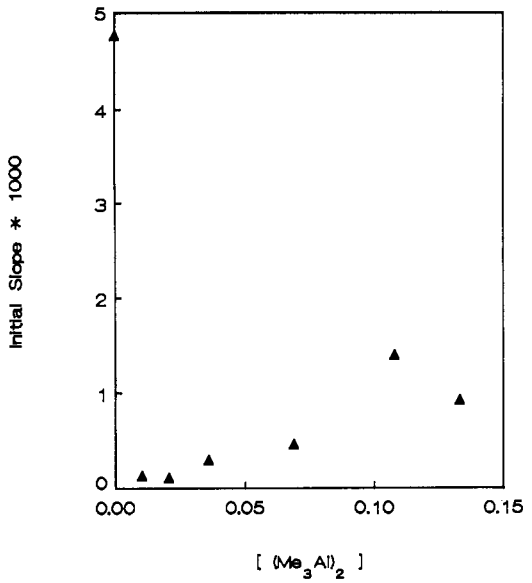

Figure 9. Influence of $[(Me_3Al)_2]$ on the initial rate of 0.081 M $Me_3Al{\cdot}NH_3$ decomposition at 55 °C.

Electrostatic interaction of the adduct's positive N–H with the N atom would be expected to make this geometry more favorable than that resulting in methane elimination. Thus methyl (and H or D) exchange would occur more rapidly than methane loss. This rapid exchange further supports the assignment of H^+ transfer, rather than methyl bridge formation, as the rate-determining step.

In addition, when $Me_3Al{\cdot}NH_3$ is added to $(Et_2AlNH_2)_3$ in D_6-benzene, ethane is rapidly evolved, and mixed trimers with complete alkyl scrambling result (compare parts A and B of Figure 2). As noted above in part C, mixing the $(Me_2AlNH_2)_3$ and $(Et_2AlNH_2)_3$ does not scramble the alkyl groups; the scrambling therefore occurs before or during alkane loss. Combining the previous mechanisms explains this.

G. Me_3Al-Catalyzed Decomposition (Paths 5 and 6). When $Me_3Al{\cdot}NH_3$ is decomposed in the presence of small amounts of $(Me_3Al)_2$ the reaction is slowed dramatically, due to suppression of the more efficient Me_2AlNH_2-catalyzed pathway. (Note the high value of the initial point in Figure 9, where $[(Me_3Al)_2] = 0$, compared with subsequent points.) An increase in the amount of $(Me_3Al)_2$ then gradually increases the rate, now due only to the less efficient Me_3Al-catalyzed route. This sharp drop followed by a gradual rise is shown in Figure 9. This is probably due to trapping of Me_2AlNH_2 to form the metastable methyl-bridged species as the kinetic product

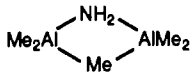

which then gradually disproportionates into $(Me_2AlNH_2)_3$ and $(Me_3Al)_2$.

The ^1H NMR spectrum of a sample of $Me_3Al{\cdot}NH_3$ that has been partially decomposed in the presence of $(Me_3Al)_2$ at 75 °C and then cooled to 50 °C is shown in Figure 10. At the temperature of decomposition, the species we believe to be $(\mu\text{-}NH_2)(\mu\text{-}Me)Al_2Me_4$ resonates at the same frequency as the $Me_3Al{\cdot}NH_3$. However, at lower temperatures, its resonance moves downfield and appears as a separate peak between those of $(Me_3Al)_2$ and $Me_3Al{\cdot}NH_3$. As the decomposition proceeds, the peak attributed to $(\mu\text{-}NH_2)(\mu\text{-}Me)Al_2Me_4$ increases and then rapidly decreases. As $Me_3Al{\cdot}NH_3$ decomposition nears completion, this peak no longer appears. The product peak initially grows very slowly as it is trapped as the intermediate and then grows rapidly as the intermediate decomposes.

This bridged species does not form when the decomposition proceeds in the absence of excess $(Me_3Al)_2$, justifying its neglect in the rate law in part D. Heating a mixture of $(Me_3Al)_2$ and $(Me_2AlNH_2)_3$ also does not generate detectable amounts of this

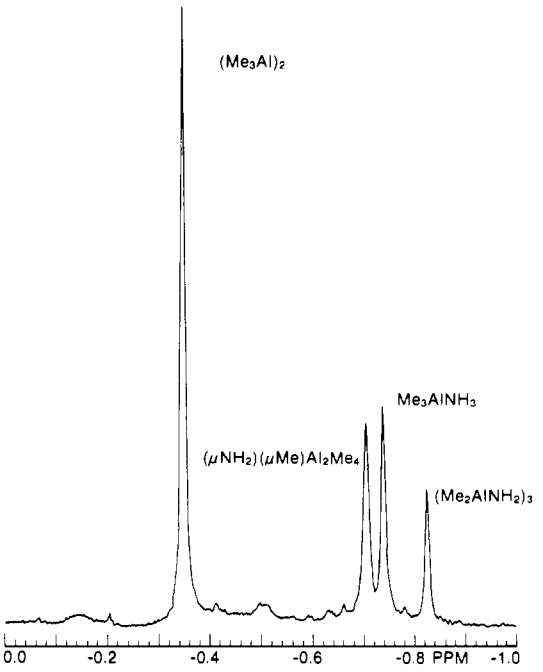

Figure 10. ^1H NMR spectrum of a solution of $Me_3Al{\cdot}NH_3$ and $(Me_3Al)_2$ in benzene-d_6, approximately half-decomposed at 75 °C and then cooled to 50 °C.

species, in agreement with the conclusions of Ziegler[38] and Schram[39] that $(\mu\text{-}NR'_2)(\mu\text{-}R)Al_2R_4$ are not stable if R′ is aliphatic. Analogous species with phenyl or trimethylsilyl R′ groups are stable.[41-44]

A solution containing 0.0824 M $Me_3Al{\cdot}NH_3$ and 0.124 M $(Me_3Al)_2$ to suppress the Me_2AlNH_2-catalyzed pathway was prepared. The initial rate of decomposition was determined at temperatures between 35 and 55 °C as described in the Experimental section. A plot of ln (slope) vs $1/T$ gave $\Delta H^\ddagger = 113 \pm 7$ kJ/mol.

An identical solution, prepared with $Me_3Al{\cdot}ND_3$ in place of $Me_3Al{\cdot}NH_3$ was also decomposed at 55 °C. The deuterium isotope effect was $R_H/R_D = 5.5$. This implies N–H bond breaking is significant at this transition state also.

We propose that Me_3Al-catalyzed decomposition of $Me_3Al{\cdot}NH_3$ proceeds via a path similar to that for Me_2AlNH_2 catalysis. The only difference is that the methyl-bridged ring formed in step D cannot rearrange to a more stable ring, because a methyl group occupies the position of the exocyclic NH_2, but instead disproportionates to $(Me_3Al)_2$ and $(Me_2AlNH_2)_3$. This mechanism is consistent with the rate law, which requires a monomeric Me_3Al catalysis, the observed isotope effect, and the metastable product formed.

The observed $\Delta H^\ddagger$ values are the sum of ΔH for production of the monomeric catalytic species and $\Delta H^\ddagger$ for the actual methane loss step. For the Me_3Al-catalyzed reaction, $\Delta H^\ddagger$ for the decomposition step is therefore 113 − 81.2 or 31 kJ/mol.

The analogous ΔH for production of monomeric Me_2AlNH_2 is unavailable. Since the NH_2 bridge is stronger than a methyl bridge, it is reasonable to expect it to be higher than 81.2 kJ/mol. Subtraction of this quantity from the observed 92.8 kJ/mol yields a $\Delta H^\ddagger$ for the Me_2AlNH_2-catalyzed step of less than 12 kJ/mol. This is plausible, as replacing a methyl group on the catalyst's Al with an NH_2 would make the catalyst a stronger Lewis acid, strengthen the Al–Me–Al bridge, and stabilize the transition state.

(38) Ziegler, K.; Kroll, W. R. *Liebigs Ann. Chem.* **1960**, *629*, 167.
(39) Schram, E. P.; Hall, R. E.; Glore, J. D. *J. Am. Chem. Soc.* **1969**, *91*, 6643.
(40) Magnuson, V. R.; Stucky, G. D. *J. Am. Chem. Soc.* **1968**, *90*, 3269.
(41) Kawai, M.; Ogawa, T.; Hirota, K. *Bull. Chem. Soc. Jpn.* **1964**, *37*, 1302.
(42) Rie, J. E.; Oliver, J. P. *J. Organomet. Chem.* **1974**, *80*, 219.
(43) Wiberg, N.; Baumeister, W.; Zahn, P. *J. Organomet. Chem.* **1972**, *36*, 267.
(44) Wiberg, N.; Baumeister, W. *J. Organomet. Chem.* **1972**, *36*, 277.

Computation of apparent $\Delta S^{\ddagger}$ values, which would represent the sum of ΔS for monomeric catalyst generation and $\Delta S^{\ddagger}$ for transition-state formation, serves little purpose in view of the unknown value of the transmission coefficient required.

H. Uncatalyzed Decomposition (Path 7). Extrapolating the data in Figure 9 to $[(Me_3Al)_2] = 0$ yields an intercept near zero. This corresponds to the rate of unimolecular Me_3AlNH_3 methane loss, assuming suppression of the Me_2AlNH_2-catalyzed pathway. Although uncatalyzed methane loss for this compound cannot be ruled out, its rate is sufficiently low that we cannot observe it.

I. Comparison with Earlier Results. For the purposes of our discussion, we write the transition state for the autocatalytic alkane loss as

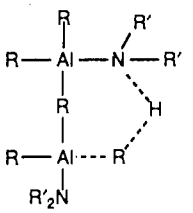

and consider the effect of altering the various groups on the rate of RH elimination, assuming that a similar mechanism to that proposed herein for $Me_3Al{\cdot}NH_3$ applies in all these cases. This is clearly an oversimplification of a complex set of observations; however, it makes possible the organization and rationalization of a substantial body of otherwise uncorrelated experimental information.

Variations at the Aluminum. (1) Changing R from methyl to ethyl, propyl, or isobutyl speeds alkane loss to such an extent that the corresponding R_3AlNH_3 adducts cannot be readily isolated.[17] This could arise from either a decreased Al–C bond strength in these compounds relative to R = Me,[45] which would facilitate the breaking of the aluminum–alkyl bond at the transition state, or from a higher concentration of the corresponding R_2AlNH_2 monomers. In the latter case, we have demonstrated that the increased steric interaction causes the corresponding dialkylaluminum amide trimers to dissociate to dimers to a much greater extent than the methyl trimer.[36] It is reasonable to suppose that there is a greater R_2AlNH_2 monomer concentration for these compounds as well, leading to more efficient catalysis.

(2) If R is H instead of Me, the reaction is speeded enormously.[46] This may be due to the much lower steric requirements of the H atom, facilitating approach by the N–H at the transition state.

(3) Replacement of methyl by *tert*-butyl slows the alkane loss dramatically.[14] This is probably due both to the poor ability of *tert*-butyl to bridge aluminum atoms and to the steric inhibition of the approach of the N–H hydrogen to the central carbon of the *tert*-butyl group.

(4) The loss of benzene when phenyl groups are on the aluminum is more difficult than methane loss,[47] in spite of the excellent bridging ability of the phenyl group. The larger expected Al–phenyl bond strength compared with Al–alkyl bond strengths would explain this.[45]

(5) Replacement of one R group by a chlorine also slows the reaction.[48] Electron withdrawal by the chlorine would make the carbon attached to the aluminum less electron rich and less attractive to the proton being transferred.

Variations at the Nitrogen. The literature data is much more extensive for Et_3Al adducts. Comparisons below are made by using the triethyl derivatives.

(1) Changing R′ from hydrogen to methyl or *tert*-butyl slows the reaction, most likely due to crowding at the transition state as suggested by Mole and Jeffrey.[49] The lower acidity of the alkyl amine would also slow the proton transfer step.

(2) If R′ is phenyl, the reaction rate is increased compared to *tert*-butyl (similar steric requirements) and when compared with hydrogen.[50] We ascribe this to the greater acidity of arylamines, facilitating H^+ transfer at the transition state.

(3) The very rapid reactions that occur when alcohols are used in place of amines is also attributable to their greater acidity.[51]

Acknowledgment. $[Me_2AlNH_2]_3$ and $[Me_2AlNHMe]_3$ were prepared by Wei Lee; $[(Et_2AlNH_2)_3]$ was prepared by Christopher Warren. Dr. Herbert Schwartz assisted with NMR measurements. We thank Drs. Corinna L. Czekaj, Johannes F. Coetzee, and Raymond Borkowski for helpful discussions, Chris Whitmarsh for assistance with the DSC measurements, and the reviewers for incisive criticism. The work was supported by the Air Force Office of Scientific Research, Air Force Systems Command, USAF, under Contract F49620-85-K-0019, and, in part, by the Chemistry Division of the Office of Naval Research. F.C.S. thanks King's College for a sabbatical leave and the NSF for participation in the NSF Summer Program in Solid State Chemistry.

(45) Skinner, H. A. *Adv. Organomet. Chem.* **1964**, *2*, 49.
(46) Reference 10, p 102.
(47) Krause, E.; Dittman, P. *Chem. Ber.* **1930**, *63*, 2401.
(48) Reference 9, p 26.
(49) Reference 9, p 230.
(50) Reference 9, p 232.
(51) Reference 9, p 212.